ENHANCED MECHANICAL AND WATER RESISTANCE PROPERTIES OF CASSAVA STARCH-PVA NANOCOMPOSITES WITH TiO2 NANOFILLERS FOR TRIBOELECTRIC NANOGENERATORS FILMS

by Aris Ansori

Submission date: 05-Apr-2023 03:48PM (UTC+0700)
Submission ID: 2056456579
File name: 2647-Article_Text-7614-1-10-20230322.pdf (5.53M)
Word count: 9542
Character count: 50495

Original Research Article: full paper

(2023), «EUREKA: Physics and Engineering» Number 2

ENHANCED MECHANICAL AND WATER RESISTANCE PROPERTIES OF CASSAVA STARCH-PVA NANOCOMPOSITES WITH TiO_2 NANOFILLERS FOR TRIBOELECTRIC NANOGENERATORS FILMS

Aris Ansori✉
Department of Mechanical Engineering[1]
Department of Mechanical Engineering[2]
arisansori@unesa.ac.id

Sudjito Soeparman
Department of Mechanical Engineering[1]

Denny Widhiyanuriyawan
Department of Mechanical Engineering[1]

Teguh Dwi Widodo
Department of Mechanical Engineering[1]

[1]*Brawijaya University*
167 MT Haryono str., Malang, Indonesia, 65145

[2]*Universitas Negeri Surabaya*
Ketintang str., Surabaya, Indonesia, 60231

✉**Corresponding author**

Abstract

The utilization of biopolymers for energy applications continues to attract researchers, due to the unique properties of biopolymers that are easily modified, such as cassava starch (CS) biopolymer that has hydroxyl molecular chains. However, the brittle, and non-waterproof nature of starch films is an obstacle to their use in triboelectric nanogenerator (TENG) solid-solid films. This study aims to improve the physicochemical properties of cassava starch films by modifying them into nanocomposite films. The nanocomposite film was made from 70:30 CS/polyvinyl alcohol (PVA) composite and variation of TiO_2 nanoparticles addition using solvent casting method. The results showed that the mechanical properties of cassava starch film increased with the addition of PVA. Meanwhile, the addition of TiO_2 above 1 wt % of the mechanical properties of the film tends to decrease. The film has low wettability properties with a contact angle of 83.6°. The performance of the nanocomposite film as a Rotary disc freestanding film (RDF-TENG) produces 4.4-fold the output voltage and 2.8-fold the current compared to the film without TiO_2. This is a new finding that the CS/PVA-TiO_2 nanocomposite film has the potential for TENG films in high-humidity environmental conditions.

Keywords: nanocomposite film, TiO_2, film properties, performance, triboelectric nanogenerator.

DOI: 10.21303/2461-4262.2023.002647

1. Introduction

Triboelectric nanogenerator (TENG) is a micro/nano energy harvesting device that converts the mechanical energy of the surrounding environment into electrical energy based on the triboelectricity effect between two materials that have different electronegativity levels and has been proven to be effective and efficient [1]. TENG working principles based on contact electrification and electrostatic induction make a self-powered system with high efficiency, low cost, abundant mechanical energy source, and high output [2, 3]. TENG was first developed in 2012, Research was conducted utilizing the triboelectric effect of materials to harvest mechanical energy into electricity and demonstrated high energy conversion efficiency [4].

TENG has become one of the promising energy conversion devices to convert mechanical energy into electrical energy due to the capacity of triboelectric materials. The TENG device

generally consists of two friction materials and electrodes at the top and bottom of the device. Physical contact between two friction materials with different levels of electronegativity can induce a triboelectric charge which can produce a potential decrease when separated by mechanical forces and increase the flow of electrons between the electrodes via an external circuit. The dominant factor that determines the performance of TENG's output is the TENG friction material, such as; the use of nanocomposite friction materials on a nanoscale which has the advantages of mechanical strength, toughness, flexibility, transparency, dielectric, thermal or electrical conductivity properties which show an effective and efficient TENG performance improvement [5, 6].

However, TENG triboelectric nanocomposite films are still dominated by synthetic polymers, which require a complicated, long, and expensive fabrication process. such as; PDMS nanocomposite films with TiO_2 deposition can cause changes in oxygen vacancies on the PDMS surface which can contribute to electron exchange and trapping and have an impact on increasing TENG output power [7], DSSC output power [8], Poly (vinylidene fluoride) (PVDF) polymer with TiO_2 NPs as filler can improve the dielectric properties [9], Polydimethylsiloxane (PDMS) with different TiO_x weight ratios as a function of dielectric constant control with 5 % rutile TiO_x and 7 % TiO_x anatase phase produces TENG output highest ~180 V/8.2 μA and 211.6 V/8.7 μA [10].

Biodegradable devices are in great demand because of the abundant raw materials available, low cost, simple process, and environmentally friendly. Various natural biodegradable materials, such as; natural rubber [11], cellulose [12, 13], chitosan, polyvinyl alcohol (PVA) [14], rice paper, and starch paper have been used to make biodegradable TENGs [15−17], and environmentally friendly raw materials and do not cause harmful effects on humans and the environment [18]. The use of starch has begun to be developed for the TENG triboelectric film because it has properties such as; biocompatible and biodegradable [16, 19–22], abundant availability, easy process, inexpensive, possessing hydroxyl groups, amorphous crystal structure, and rheological properties can provide the required resistance for TENG triboelectric film applications [23].

Meanwhile, previous studies showed high performance of TENG based on starch biofilm, such as; TENG-based, due to the binding of water molecules and hydroxyl groups through hydrogen bonds [21]. TENG-based potato starch biofilm exhibits high output voltages from 60 mV to 300 mV per 4 cm^2 area, but the surface of the film is prone to cracking at several duty cycles [22]. Tapioca starch film rich in hydroxyl groups can enhance the triboelectric effect by binding water molecules on the friction film surface through hydrogen bonding [24]. The use of starch polymer electrolyte film made from a mixture of potato starch and 0.5 % $CaCl_2$ showed an increase in voltage output three times higher than pure starch from 0.4 V to 1.2 V. Starch polymer electrolyte between potato starch and 0.5 % $CaCl_2$ showed an increase in voltage output three times higher than pure starch from 0.4 V to 1.2 V [19].

However, the strong hydrophilicity of starch causes poor mechanical properties and easily soluble in prolonged contact with water. This becomes a bottleneck for starch films for TENG biodegradable applications that require long-term stability. Therefore, to increase the functionality of starch by modifying starch into nanocomposite films. In this study, we fabricated a starch-based nanocomposite film, by synthesizing cassava starch/PVA-TiO_2 into a nanocomposite film. Our knowledge, the use of TiO_2 as a filler in starch composites to improve mechanical properties and water resistance for Biodegradable TENG has never been reported. Meanwhile, the addition of PVA to starch polymers as a composite matrix can help the formation of polymer composite bonds through hydrogen bonding and increase the number of hydroxyl groups [25]. The use of TiO_2 nanofiller which is an inorganic nanoparticle with a large specific surface area and high surface energy can result in some –OH groups or dangling bonds contained in the biopolymer matrix that can be adsorbed on the nano-TiO_2 surface, which can affect the physical characteristics of the natural polymer/composite properties. In addition, the formation of hydrogen bonds and C-O-Ti bonds between starch matrices and TiO_2 can help the dispersion of TiO_2 as a filler in starch matrices which can improve the compatibility between starch and TiO_2 [26].

Meanwhile, the special emphasis of this study is to investigate the effect of TiO_2 in CS/PVA polymer blends on mechanical properties, water resistance, and TENG characterization with CS/PVA-TiO_2 nanocomposite films as positive friction surfaces. We analyze the performance

TENG of CS/PVA-TiO_2 nanocomposite films and the changes in properties of CS/PVA nanocomposite films with different concentrations of TiO_2 nanofillers.

The improvement in tensile strength and elongation at break of CS/PVA composite films is due to the high mechanical properties of PVA. In addition, the water resistance property was improved with the formation of more OH groups. Meanwhile, the effect of TiO_2 addition in CS/PVA composite increases the rigidity of the molecular chain with the help of hydrogen and covalent bonds, the elasticity of the molecular chain decreases which causes the elongation at break value to tend to decrease with the increase of TiO_2 concentration in the CS/PVA matrix. The presence of TiO_2 makes the more dense film, thus increasing the absorption of water molecules so that the film is not easily damaged.

Meanwhile, the performance of RDF-TENG nanocomposite CS/PVA film produced an output voltage and current of ~25.5 V and ~3.6 μA. The effect of TiO_2 addition on the performance of RDF-TENG film of CS/PVA-TiO_2 nanocomposite was optimally improved by the addition of 3 % TiO_2 that resulted in 4.4 times the output voltage and 2.8 times the current compared to the TENG film of CS/PVA without TiO_2 nano-filler. Therefore, these CS/PVA-TiO_2 nanocomposite films have the potential for TENG films under high-humidity environmental conditions.

2. Materials and methods

2. 1. Materials

Materials starch used in the experiment is cassava starch produced by PT. Budi starch & Sweetener. Tbk. in Indonesia, Polyvinyl Alcohol (PVA) with an average molecular weight of $Mw = 89.000–98.000$, was procured from Sigma Aldrich, Anatase TiO_2 nanoparticles with a particle size of 20 nm were purchased from Sigma-Aldrich, glycerol (99 % purity, clear, colorless, and density: 1.261 g/cm^3) from Merck, distilled water specification; PH 8, resistivity >200 KΩ, conductivity <5 μS/cm, Copper tape type dual side conductor (adhesive side and conductive outside side) and thickness 0.5 mm.

2. 2. Preparation of cassava starch (CS)/PVA-TiO_2 nanocomposite

Fig. 1 describes making cassava starch (CS)/PVA-TiO_2 nanocomposite using the solvent casting method.

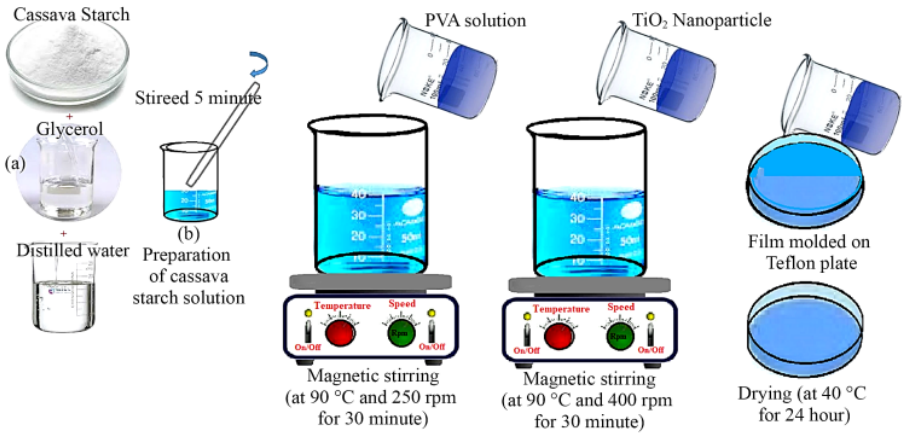

Fig. 1. Preparation of CS/PVA-TiO_2 nanocomposite films

Preparation of CS/PVA-TiO_2 nanocomposite films by solvent casting method as shown in **Fig. 1** by steps:

a) making a solution of cassava starch (CS), with a composition of cassava starch (4.2 g), and glycerol (3 g) as plasticizer dispersed with distilled water (50 mL) in borosilicate glass;

b) The solution of cassava starch (CS), and glycerol was mechanically stirred for 5 minutes until the solution was completely homogeneous;

c) cassava starch solution (CS) was stirred with a magnetic stirrer at a speed of 250 rpm at a temperature of 95 °C for 30 minutes to obtain a gelatinized starch suspension and added PVA solution while stirring continuously (250 rpm) for 30 minutes until it dissolved completely and a clear solution was formed;

d) CS/PVA clear solution was added with TiO_2 nanoparticles (0.5, 1, 3, 5, 7 % wt.);

e) CS/PVA-TiO_2 nanocomposite films were cast with a Teflon mold diameter of 100 mm;

f) the drying of the film was carried out in a hot air oven at 40 °C for 24 hours. Meanwhile, the composition ratio of Cassava starch (CS), PVA, and TiO_2 for nanocomposite film samples are presented in **Table 1**:

Table 1

Composition of The Various Film Nanocomposite Samples

Nanocomposite Sample	Composition		
	Cassava strach (CS)	PVA	TiO_2 (% wt.)
CS-PVA	70	30	0
CS-PVA/0.5 TiO_2 % wt.	70	30	0.5
CS-PVA/1 TiO_2 % wt.	70	30	1
CS-PVA/3 TiO_2 % wt.	70	30	3
CS-PVA/5 TiO_2 % wt.	70	30	5
CS-PVA/7 TiO_2 % wt.	70	30	7

First, to determine the constant weight ratio of the CS/PVA mixture (70:30), cassava starch (4.2 g) was dispersed with distilled water (50 mL) in borosilicate glass, the addition of glycerol (3 g) served as a plasticizer and mechanical stirring was carried out until completely homogeneous. Furthermore, stirring with a magnetic stirrer at 250 rpm at a temperature of 95 °C for 30 minutes to obtain a gelatinized starch suspension. Meanwhile, in another borosilicate glass, the PVA solution was prepared by dissolving 1,8 g of PVA with 40 mL of distilled water and mechanically stirring (250 rpm) for 5 minutes, then the temperature was gradually increased to 95 °C and continuously stirred (250 rpm) for 30 minutes until completely dissolved and a clear solution is formed. Mixing of the two solutions (gelatinized CS suspension- PVA suspension) was carried out at room temperature and continued to be stirred with a magnetic stirrer (250 rpm, 95 °C).

Furthermore, the PVA solution, cassava starch suspension, and TiO_2 (0,5 %, 1 %, 3 %, 5 %, and 7 % wt.) (**Table 1**) particle dispersion (CS/PVA-TiO_2) were combined and stirred continuously at 400 rpm and a temperature of 95 °C for 30 minutes using a magnetic stirrer. The solution was in a vacuum for 10 minutes using vacuum machine to remove residual air from the solution. The viscous solution produced from the CS/PVA-TiO_2 polymer was poured into a Teflon mold (radius 50 mm). when pouring, the volume of the polymer mixture in each mold was controlled constant, producing relatively the same thickness as the nanocomposite film sample. The drying of the film was carried out in a hot air oven at 40 °C for 24 hours. The dry film was then carefully peeled off from the Teflon mold and produced a film with an average thickness of 100 µm. The resulting nanocomposite films were kept in a zippered bag until tests were carried out to reduce water absorption according to the Ramirez method [27].

2. 3. Fabrication of rotary disk freestanding (RDF-TENG)

The rotary disk freestanding TENG (RDF-TENG) structure consists of two parts, rotor and stator. Rotor structure parameters with the number of film segments (n) = 4, outer radius (r_2) = 50 mm, inner radius (r_1) = 5 mm, and made of commercial polyimide thin film (0.03 mm) as a triboelectric film glued to an acrylic surface (radius = 50 mm). Meanwhile, the stator structure parameters consisting of CS-PVA/TiO_2 nanocomposite films were cut to form an equal interval electrode model with the number of film segments (n) = 8, outer radius (r_2) = 50 mm, inner

radius (r_1) = 5 mm, and the nanocomposite film thickness was 100 μm. Next, the cut nanocomposite film was glued to the copper foil (electrode film A, and B). Where the tip of the copper foil electrode is slightly exaggerated to connect the external circuit with the help of a conducting wire so that electrons can flow into the external circuit. External mechanical energy uses a DC electric motor that is connected to the TENG rotor shaft in a freestanding rotational mode. Meanwhile, the gap between the rotor and stator was controlled with a distance of 0.10 mm to keep the friction between the surface of the polyimide film and the CS/PVA-TiO_2 nanocomposite film stable. The design and structure of RDF-TENG with cassava starch/PVA-TiO_2 nanocomposite films are presented in **Fig. 2, *a***.

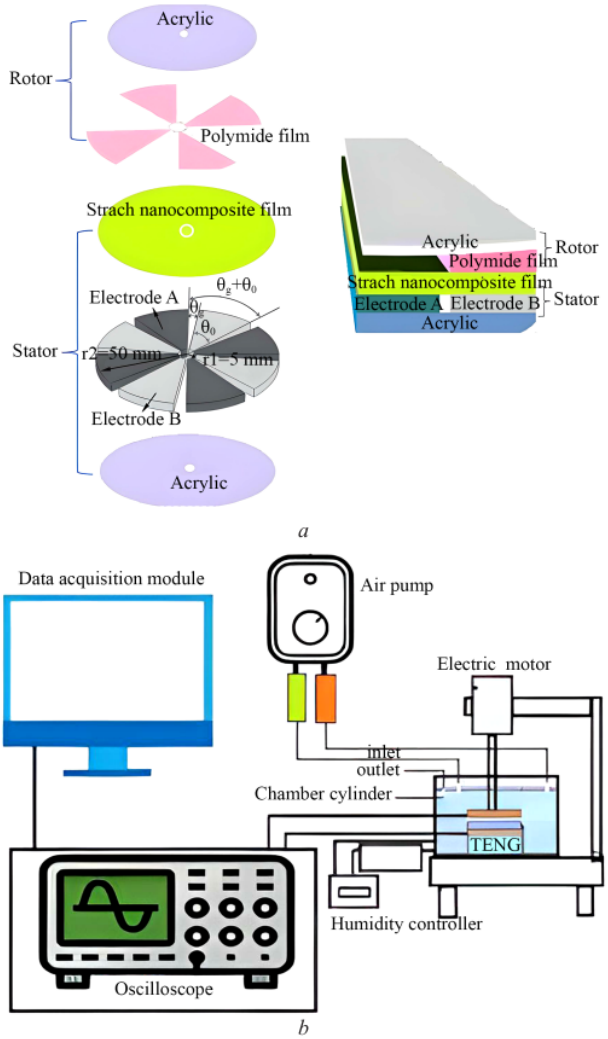

Fig. 2. RDF-TENG testing and structure: *a* – RDF TENG array, *b* – TENG testing instrument

The schematic diagram of the TENG output test mechanism is shown in **Fig. 2, *b***. Conditioning for humidity levels of 15 % and 95 % were carried out by placing the TENG in a closed cylindrical chamber. The operating Rotary-disk freestanding (RDF-TENG) mode consists of a rotor with four electret sectors attached to a dielectric substrate using a polyimide film.

The stator is composed of six sectors of a CS-PVA/TiO_2 nanocomposite film connected to a copper foil electrode. Distance between the rotor and stator surfaces with an air gap of 0.10 mm.

2. 4. Characterizations of cassava starch/PVA-TiO_2 nanocomposite films

2. 4. 1. Chemical, structural, and morphological analysis

Surface analysis and morphology of starch/PVA-TiO_2 nanocomposite films using Scanning Electron Microscope (FESEM) FEI Quanta FEG 650. The dry film sample was sprayed with gold-palladium under vacuum conditions to increase its conductivity. The test was carried out at a voltage of 15xKV with a magnification of 500x, and 10Kx. The functional groups of the nanocomposite films were analyzed using Fourier transform infrared spectroscopy (FTIR) with an IRPrestige-21 spectrophotometer (Shimadzu, USA). FTIR measurements were carried out at room temperature (25 ± 10 °C) in the wave number range of 600–4000 cm^{-1} with a resolution of 2 cm^{-1} and an average of more than 32 scans. The X-ray diffraction (XRD) analysis to determine the crystalline atom form of starch/PVA-TiO_2. The degree of crystallinity of the film samples was recorded using a PAN analytical Xpert Pro diffractometer with Cu Kα radiation at 40 kV and 40 mA, using a 20 mm Ni filter. All sample films were scanned between 2θ = 5° to 69.99° at 5°/min measurement Temperature of 25 °C.

2. 4. 2. Mechanical properties

Testing the mechanical properties of the film consists of tensile strength (Ts), Elongation at break (Eb), and Young's Modulus (My). Testing according to the ASTM standard method D882-10 (ASTM, 2010) using the Tensile Testing Machine. The samples film (length×width×thickness = 100×20×5 mm) was conditioned at RH = 55 % for 48 hours. Next, each film sample was mounted between the machine's grips and tested at a crosshead speed of 5 mm/min at room temperature (23 °C) [28].

2. 4. 3. Water-resistance

Water resistance testing was conducted to identify the degree of water damage to the film. The film samples (length×width×thickness = 100×20×0.5 mm) were immersed into beakers filled with distilled water. The immersion time of each film sample until the film texture was damaged (destroyed) in the water. The results of recording the immersion time of the film sample were used to determine the level of resistance of the film sample to water.

2. 4. 4. Water contact angle

Measurement of the contact angle of the nanocomposite film was carried out to determine the level of wettability of the film surface to water. The sample contact angle was measured using a contact angle goniometer (Rame-Hart Instrument C, USA). The film sample (length×width×thickness = 25×25×0.5 mm) was placed horizontally on the contact angle measuring bench by the sessile drop method [29]. Drops of 4 µL deionized water were placed on the film's top surface. droplet images and contact angle values are recorded from the software 20 seconds after deposition. The contact angle is calculated using a mathematical equation with the shape of a water droplet and calculates the tangent line between the water droplet and the solid film. For each film sample, 5 readings were taken at different film locations.

2. 4. 5. Electrical output measurement

TENG output performance measurement using freestanding rotary mode. The rotating mechanical energy of the DC motor is used to rotate the TENG rotor. To measure the TENG output voltage and current, the TENG rotor is energized externally by the DC motor rotation. The rotation is controlled at 200 rpm using a controller that regulates the electric current entering the DC electric motor. The rotation of the rotor on the stator causes friction on the surface of the polyimide film and the CS-PVA/TiO_2 nanocomposite film causing a triboelectricity effect. The electrode poles of films A and B were measured output voltage and current using a digital oscilloscope (DSOX6004A Digital Storage Oscilloscope) with a load resistance of 100 MΩ. Meanwhile, the TENG output performance test based on CS-PVA/TiO_2 nanocomposite films

under different humidity conditions was carried out in a cylindrical chamber, before the testing film was put in a closed box for 24 hours with adjusted humidity control (RH 15 %, and 95 %) with a saturated salt solution. Furthermore, testing the output performance of TENG in the same humidity control box was carried out in a closed cylindrical chamber, a cylindrical chamber equipped with two inlets and one outlet. Where the first inlet drains dry air (located on the right), and the second inlet drains moist air (located on the left). Meanwhile, the outlet is used to control air circulation in the cylinder (located on the left). This control mode can accurately achieve the required relative humidity in the room.

3. Results and discussion

3. 1. Chemical, structural, and morphological analysis of the cassava starch-PVA/TiO_2 nanocomposite film

Structural analysis can be observed from the FTIR spectrum of the material in the range of 4000–700 cm^{-1}. Where the molecular bond spectra of the CS/PVA polymer matrix and the change after incorporation of TiO_2 filler, which has several characteristic peaks, reflect the structure of the two biopolymers. The transmittance band of about 3285 cm^{-1} was determined from the stretching vibration of the hydroxyl group (–OH) in CS and PVA polymers having a hydroxyl-rich average. The peak transmittance band of 1641.42 cm^{-1} indicates the formation of hydrogen bonds in pure starch due to the flexion of the –OH molecule and shows the hygroscopic nature of the starch polymer. Characteristics of the bending of C-OH in the 1205 cm^{-1} transmittance band. The peak at 770–1120 cm^{-1} is associated with the stretching of the C–O bond of the macromolecular portion, where an intramolecular hydrogen bond is formed between two adjacent OH groups that are on the same side of the plane of the C–C carbon chain of the C–O–C group of the unit. glucose in starch [30].

Pure PVA showed hydroxyl and acetate groups, where the intermolecular and intramolecular hydrogen –OH bonds were shown in a wider band at 3296.35 cm^{-1}.

The structure of the alkaline group confirmed the peak in the transmission band 1480–1190 cm^{-1} associated with the planar buckling vibrations of C–H and O–H in both CS and PVA. The presence of a carbonyl group (C = = O) is indicated by the 1732 cm^{-1} transmission band and a hydrocarbon (alkane) group in PVA is indicated by a peak at 1373.32 cm^{-1} [31]. Meanwhile, the chemical interaction between CS/PVA polymer molecules that causes changes in the characteristic spectral peaks of the composite, the C-OH hydrocarbon group is estimated to come from the C-O vibrations, which are confirmed by the peak of 1000–1250 cm^{-1}. In addition, the vibration of the –OH group confirmed the absorption peak in the range of 3300–3000 cm^{-1}. The formation of the C–H alkene functional group due to the mixing of CS/PVA which was confirmed at a wavelength of 675–995 cm^{-1} and C-H alkane which was confirmed at a wavelength of 2850–2970 cm^{-1}.

In addition, the C-H functional group of the aromatic ring was confirmed at the wavelength of 690–900 cm^{-1}. The mixing of CS/PVA polymer showed flexural vibrations of the hydrogen bonding of the –OH group at 1710.86 cm^{-1} and the C–O strain at 1050–1300 cm^{-1}. The stronger interaction of CS/PVA molecules is shown by intermolecular interactions through the formation of hydrogen bonds with water vapor molecules, which can increase triboelectricity. At low concentrations (below 7 % TiO_2 wt.) in the CS/PVA polymer mixture in the FTIR spectrum, the vibration peaks did not show any additional peaks. This may be due to the overlapping bands of the CS/PVA components. However, the increase in TiO_2 concentration (above 1 % TiO_2 wt.) showed a slight shift in the peak positions of several bands in the range of 900–1100 cm^{-1}. It is assumed that the absorption band at 1000 cm^{-1} is associated with the TiO_2 crystal domains hydrated into the CS/PVA polymer matrix. In addition, the titanium ions of the TiO_2 particles can interact with the hydroxyl groups of CS/PVA, which make the nanocomposite films highly compatible. The results of the FTIR test for each concentration of TiO_2 nanofiller in the cassava starch/PVA composite are presented in **Fig. 3**.

The results of the XRD test for each concentration of TiO_2 nanofiller in the cassava starch/PVA nanocomposite are presented in **Fig. 4**. Shows the XRD pattern of the sample film, the cassava starch film produced peaks at $2\theta = 15.73°$, 16.51°, 17.23°, 19.69°, 22.14°, and 24.37°. Whereas, an important diffraction peak located at 19.69° which indicates strong intermolecular and intramolecular hydrogen bonds, and is indicative of a semi-crystalline structure, this is not much

different from the signal of the 20°peaks of cassava starch [32]. Meanwhile, the CS-PVA composite sample formulation produced peaks at 2θ = 13.11°, 17.21°, 19.76°, and 24.54°, which indicated a change in peak. These peaks can reveal that polymer cassava starch (CS) is dispersed in PVA which can change the characterization of the films [33, 34]. The incorporation of TiO_2 filler into CS/PVA with variations in TiO_2 concentration below 1 % wt. showed peak changes that were not easily visible at low concentrations. However, increasing the concentration above 1 % by weight showed peaks at 2θ = 22.38°, 27.60°, and 54.43° in semicrystalline structure nanocomposite films and indicated the presence of titanium dioxide embedded in the CS/PVA polymer.

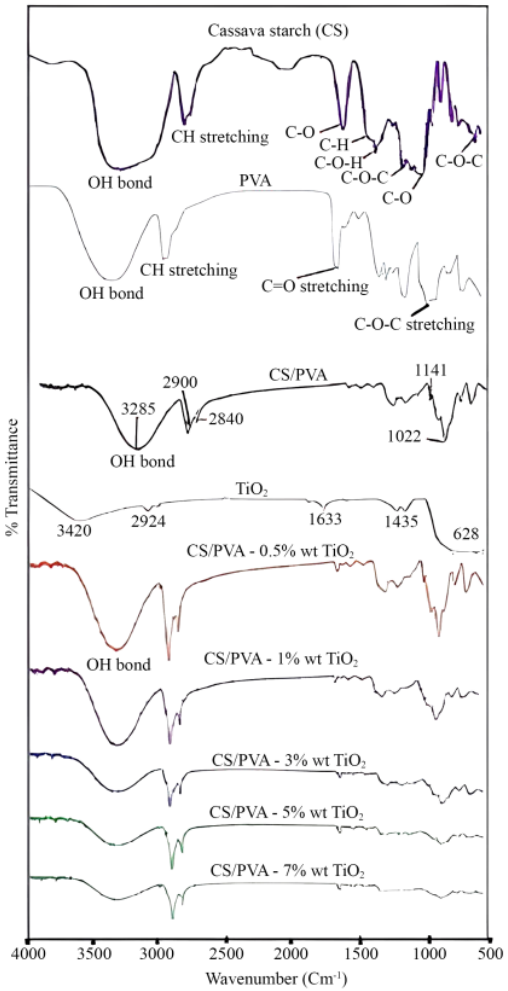

Fig. 3. Chemical formula analysis of cassava starch/PVA-TiO_2

The morphology of the polymer mixture of cassava starch (CS)/PVA and the morphological changes of the nanocomposite films after the addition of TiO_2 can be observed from the material micrograph. The ability of starch granules to interact with various ceramic and mineral particles can hold these particles, which causes the added TiO_2 to adhere to the surface of the starch granules well. Meanwhile, mixing CS/PVA suspension with TiO_2 particles, during the gelatinization process, the TiO_2 particles remain attached to the surface of the starch granules and interact with

the continuous phase macromolecules of water-soluble amylose and PVA, this process most likely occurs through hydrogen bonding. SEM photographs show the morphology of each film sample appears to have a heterogeneous surface relief (**Fig. 5, *a***).

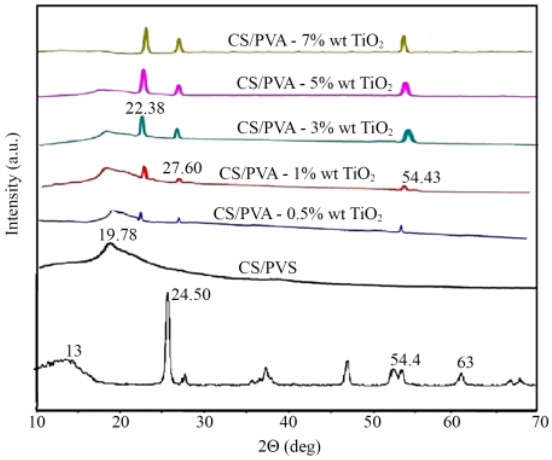

Fig. 4. XRD patterns for TiO_2 nanoparticle, CS/PVA, and CS/PVA-TiO_2 nanocomposite

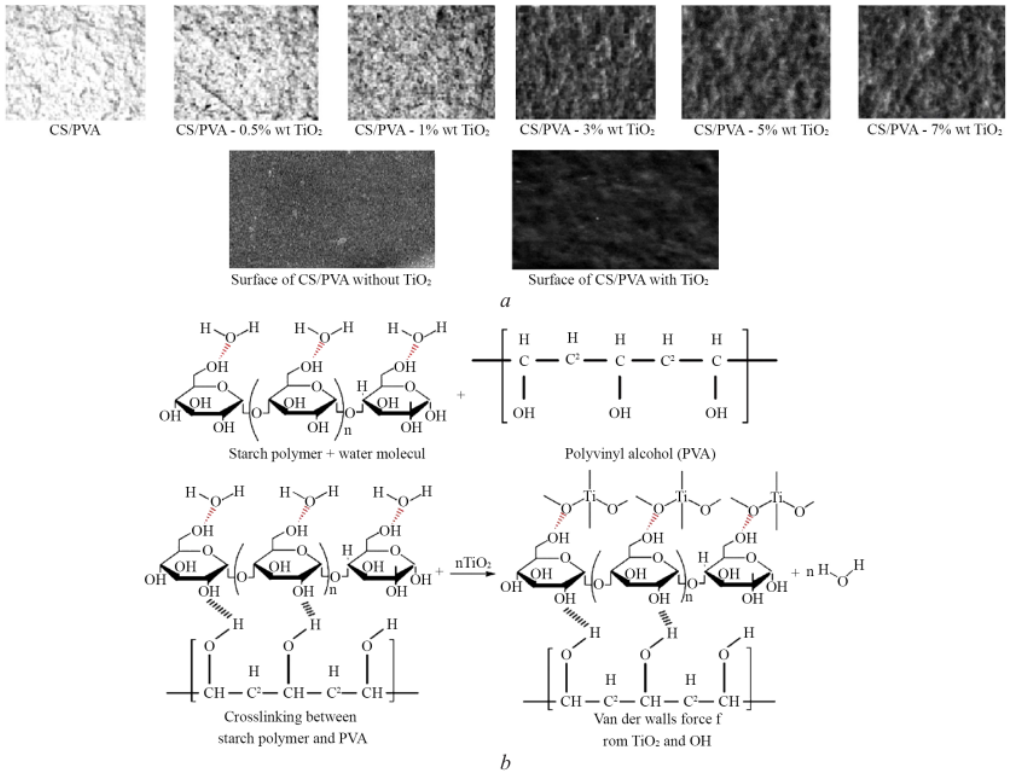

Fig. 5. Morphology surface and reaction between TiO_2 and polymer OH: *a* – surface photographs of CS/PVA without TiO_2 and with TiO_2; *b* – hydroxyl groups adsorbed on nano-TiO_2 surface

The CS/PVA blend film had a small amount of agglomeration, but the agglomeration formed was not very obvious. This is due to the strong interaction between the molecules of the CS/PVA blend and the compatibility of the CS/PVA blend. Meanwhile, the addition of TiO_2 nanoparticles to CS/PVA composites showed an increase in agglomeration formation. The addition of 7 % wt. TiO_2 nanoparticles to the CS/PVA composite showed the most agglomeration of TiO_2 and was clearly visible. This increase in agglomeration is due to the inert nature of TiO_2 as a filler of CS/PVA composites. Significant nano-TiO_2 agglomeration can affect the surface roughness of the nanocomposite film. The positive effect of the surface roughness of the nanocomposite film can be beneficial in improving the charge transfer on the friction surface when applied as a triboelectric nanogenerator (TENG) friction film. Furthermore, the possibility of TiO_2 nanoparticles with large specific surface area and high surface energy as a filler material for polymer composites may cause some –OH groups in the biopolymer matrix to be adsorbed on the surface of nano-TiO_2 which can help the dispersion of TiO_2 particles in CS/PVA composites through van der walls force (**Fig. 5, *b***). Whereas, this is in contrast with the addition of TiO_2 concentration of more than 1 % wt. indicating the association of filler particles in the composite. In addition, the presence of TiO_2 particles with a high ratio in the film can create a winding path that prolongs the transport of water vapor molecules.

3. 2. Mechanical properties

To analyze the performance of CS/PVA-TiO_2 nanocomposite films related to mechanical viability, tests were carried out which included; Tensile Strength (T_S) is the maximum tensile stress that the material can sustain before failure, Young's modulus (M_y) is the level of elasticity of the material under longitudinal traction, and elongation at break point (E_B) is a measure of the elasticity of the material. The results of the study of mechanical properties (**Table 2**) show that the tensile properties of the CS/PVA composite film are very good with 14.23 MPa and elongation at break point of 112.13 %.

Table 2

Mechanical Characterization of Nanocomposite Film

Composite Sample	Mechanical Characterization		
	Ultimate Tensile Strength (T_S), MPa	Elongation at break (E_B), %	Young's Modulus (M_y), MPa
CS-PVA	14.23±2.25	112.13±2.28	70.27±4.12
CS-PVA/0,5 TiO_2 % wt.	19.11±1.35	80.45±9.25	113.38±4.57
CS-PVA/1 TiO_2 % wt.	21.20±2.52	78.20±17.12	75.45±6.59
CS-PVA/3 $TiO_{2\,\%}$ wt.	10.13±1.26	81.43±4.22	73.27±8.53
CS-PVA/5 $TiO_{2\,\%}$ wt.	9.27±1.60	76.23±2.55	75.83±8.12
CS-PVA/7 $TiO_{2\,\%}$ wt.	9.50±1.75	73.23±15.54	74.76±9.35

The mechanical properties of CS/PVA composites are good due to the high mechanical properties of PVA due to the flexible C–C and a large number of –OH groups. In addition, the interaction of the –OH group of both CS and PVA polymers through hydrogen bonds makes good compatibility between CS and PVA polymers. So far, the results of previous studies reported that decreasing the concentration of PVA polymer in starch/PVA composites decreased the mechanical properties of the films [35, 36]. Meanwhile, the incorporation of TiO_2 particles into the CS/PVA composite showed a significant increase in the Tensile Strength value for the CS/PVA/TiO_2 film sample – 0.5 % wt. increased from 14.23 MPa to 19.11 MPa. While the addition of TiO_2 – 1 % wt. showed the optimal Tensile Strength of 21.20 MPa. However, the effect of TiO_2 on the CS/PVA composite caused the elongation at break value of the CS/PVA-TiO_2 nanocomposite to decrease. On the other hand, the addition of TiO_2 nanoparticles above 3 % wt. shows that the Tensile Strength tends to decrease and the elongation at break tends to decrease. The possibility of adding more than 3 % wt. of nanoparticles causes TiO_2 particles to agglomerate and spread unevenly. where these

results are in line with research reported by previous researchers [30], besides, the concentration of filler material can increase the adhesion strength of the material [37, 38]. The improvement of mechanical properties of cassava starch/PVA-TiO_2 nanocomposite films was in line with previous studies using a variety of fillers on starch/glycerol/Li composite films [30], and starch-sisal fiber [39]. In addition to fillers, the effect of using glycerol also has an impact on the properties of elongation at the break [33, 40], and effect of TiO_2 nanoparticles on barrier and mechanical properties effect of TiO_2 nanoparticles on barrier and mechanical properties [29, 41−49]. The results of testing the mechanical properties of the film with variations in the percentage of TiO_2 content were 0.5 %, 1 %, 3 %, 5 %, and 7 % are presented in **Table 2**.

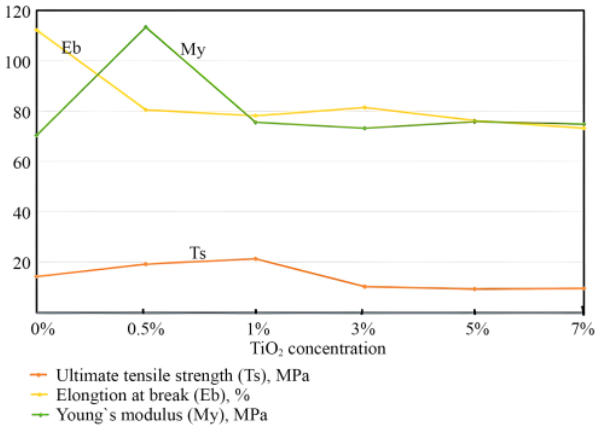

Fig. 6. Comparison of Ts, Eb, and My values of CS/PVA-TiO_2 nanocomposite films due to different concentrations of TiO_2

3. 3. Water-resistance of CS/PVA-TIO_2 nanocomposite films

The water resistance test of CS/PVA-TiO_2 nanocomposite films aims to determine the degree of film damage when interacting with water molecules. The test method and results of water-resistance testing of nanocomposite films are presented in **Fig. 7**. To determine the water resistance of CS/PVA-TiO_2 nanocomposite films, it was carried out by immersing the nanocomposite films in cylindrical beaker filled with distilled water. Dimensions of the film tested $L \, x \, w \, x \, h$ (30×20×0.01 mm). The immersion film was carried out until the film texture was damaged and crushed, as presented in (**Fig. 7, *a***). The water resistance test results of the films are presented (**Fig. 7, *b***), the water resistance of CS/PVA nanocomposite films with TiO_2 nanofiller increased 2-fold compared to that without TiO_2, where the water resistance of the CS film for 17 hours, CS/PVA increased for 20 hours, and the optimal water resistance of the SC/PVA-TiO_2 nanocomposite film for 32 hours with the addition of 7 % by weight of TiO_2. The resistance of CS films is influenced by the number of hydroxyl groups in the polymer molecule, where the hydroxyl groups bind to water molecules by forming hydrogen bonds. The increase in the number of hydroxyl groups in the CS/PVA film can occur from the intramolecular interaction of the CS/PVA polymer mixture, which can significantly increase the binding of water molecules. Meanwhile, the waterproof properties of CS/PVA-TiO_2 nanocomposite films can be due to the influence of hydroxyl groups that bind water molecules through hydrogen bonds. In addition, the presence of TiO_2 in the CS/PVA polymer mixture makes the film denser, thereby increasing the absorption capacity of water molecules. On the other hand, TiO_2 also has hydrophobic properties, which can slow down the absorption of water molecules on the surface film. This result is not much different from the results of previous research reports, the effect of TiO_2 nanofiller in polymer films causes a decrease in moisture penetration of corn starch/PVA-TiO_2 films [30], Potato Starch/Montmorillonite-TiO_2 composite films [30], Potato starch/lactucin-TiO_2 composite films [42].

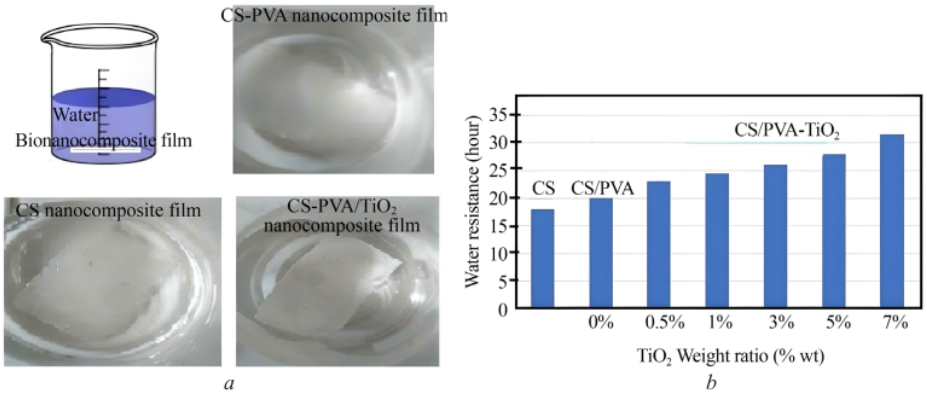

Fig. 7. Methods and analysis of water resistance: *a* – film testing method; *b* – results of water resistance testing of CS/PVA-TiO_2 nanocomposite films

3. 4. Water contact angle

Water contact angle measurements were carried out to evaluate the wettability of the surface of the film against water molecules. The CS/PVA composite film sample yielded a value of 69.9° indicating hydrophilic properties.

The hydrophilic properties increased due to the increase in polar groups such as C–O and –OH due to the mixing of PVA polymer with water-soluble properties. This increase in the –OH group increases the ability to form hydrogen bonds with water molecules resulting in higher wettability. The decrease in the water contact angle on the surface of the starch/PVA film was in line with previous studies, which was caused by an increase in the hydroxyl chains [30, 33, 36]. Meanwhile, the addition of TiO_2 to the CS/PVA composite with the addition of 0.5 % wt. to 7 % wt. TiO_2 nanoparticles showed a trend of increasing the contact angle of the film surface (70.8°, 71.1°, 74.3°, 77.5°, 83.6°) (**Fig. 8**). The increase in contact angle was due to the distribution of TiO_2 particles on the surface of the CS/PVA-TiO_2 nanocomposite films. The increase in the coarser surface structure of the film is the basis for increasing the hydrophobicity of the film. where, the results of this study are in line with previously reported studies [29, 44].

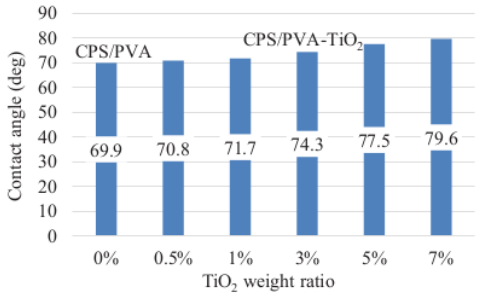

Fig. 8. The water contact angle of CS/PVA nanocomposite film vs CS/PVA-TiO_2 nanocomposite film

3. 5. Performance TENG of CS/PVA-TiO_2 nanocomposite films

The TENG current output mechanism can be divided into three stages (**Fig. 9**). In the first stage, at the initial position, the electrode A is parallel to the electret. In the second stage, the electret rotates the position of electrode A and electrode B parallel to the electret causes the charge on electrode A to be transferred to electrode B through an external load (resistor) and generate current and voltage across the load resistor during this working period. The third stage is the final state

where electrode B is parallel to the electret. While the TENG output circuit uses a rectifier diode and a capacitor as electrical storage to convert AC to DC before being channeled to the ED load.

TENG performance measurements (**Fig. 9**) were carried out at different humidity levels (15 %, and 95 %), the rotor rotation speed was controlled sTable ($\omega = 200$ rad/s), and the load was 50MΩ. TENG output performance test with CS-PVA triboelectric film without TiO_2 at low humidity level (RH, 15 %), as shown in (**Fig. 10**). The results of the output voltage and current output voltage and current ~25.5 V and ~3.6 μA without addition of TiO_2 in CS-PVA nanocomposite matrix, are presented in (**Fig. 10, *a*, *b***). Meanwhile, the addition of TiO_2 in the weight ratio (0 % to 7 % wt. TiO_2) showed a linear increase in voltage and current, respectively, as shown in (**Fig. 10, *a*, *b***). The optimal output voltage and current were achieved at a concentration of 3 %wt TiO_2 with a value of 112.5 V and 10.2 μA. This increase in output voltage and current is due to an increase in the value of the dielectric constant due to the presence of TiO_2 in the CS-PVA polymer mixture which can increase the triboelectric of the film. These results show similarities with some of the results of previous research reports, such as; an increase in dielectric properties of Poly (Vinylidene Fluoride) film with TiO_2 NP deposition [9], TiO_2 doping on Portland Cement [42], Dielectric constant changes linearly as a function of weight ratio of PDMS embedded TiO_x NP [10], natural rubber (NR)-TiO_2 [11].

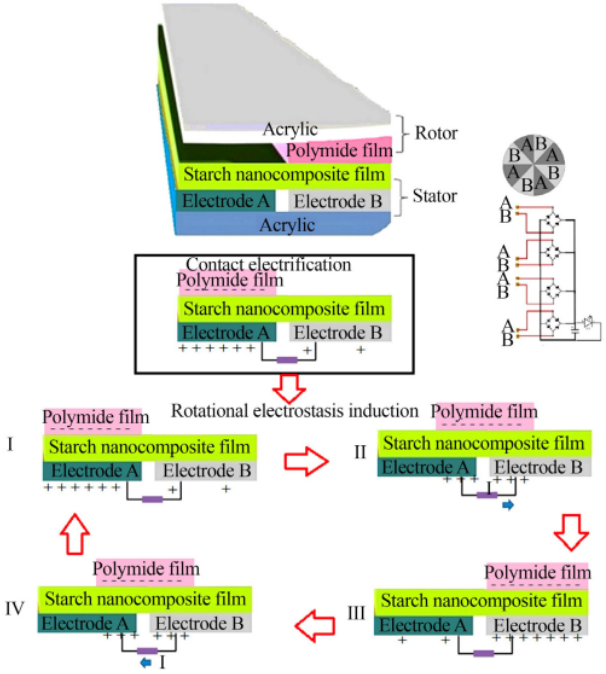

Fig. 9. Measurement of rotary disc freestanding TENG (RDF-TENG) with electrode components A, and B using copper tape thickness 1 mm, and electronic components (bridge diode 1 A 500 V), electrolytic capacitor 1000 uF 16 V, Light Emitting Diode lamp voltage 2.5 V

In addition, the effect of differences in relative humidity factors (RH, 15 %, and 95 %) on the output performance of CS/PVA-TiO_2 film-based TENG at a weight ratio above 3 % TiO_2 shows that the resulting voltage and current increase are directly correlated with increased humidity levels (**Fig. 10**). The output performance of TENG when the relative humidity condition 15 % showed an output voltage ~112.5 V and current ~10.2 μA (**Fig. 10, *a*, *b***). Enhanced relative humidity of the cylinder chamber is carried out by continuously injecting wet air into the closed cylinder chamber to increase the humidity 95 % (as shown in **Fig. 9**). Under conditions of relatively high

humidity (95 %), TENG can produce ~180 V and current from ~13.7 μA. However, the TENG output voltage and current increase was lower at a TiO_2 weight ratio of less than 3 %, as shown in (**Fig. 11**). Meanwhile, the increase in TENG optimal output voltage and current when humidity is high (RH, 95 %) with a concentration of 7 % wt. TiO_2 can reach 1.6-fold from ~112.5 V to ~180 V, and the current increases 1.4-fold from ~10.2 μA to ~13.7 μA (**Fig. 10**), and (**Fig. 11**). The output voltage and current of RDF-TENG when the humidity is 15 % are presented in **Fig. 10**, and the humidity is 95 % are presented in **Fig. 11**.

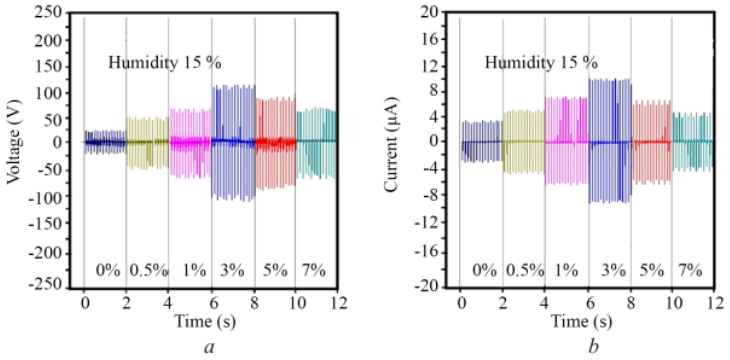

a *b*

Fig. 10. Performance RDF-TENG at humidity 15 %:
a – open circuit output voltage (V_{oc}); *b* – closed circuit output current (I_{sc})

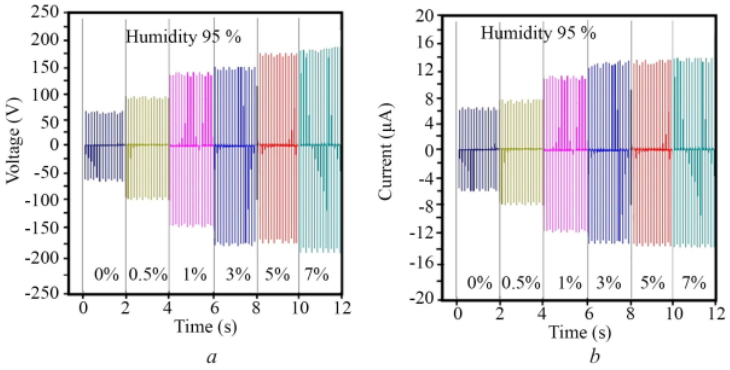

a *b*

Fig. 11. Performance RDF-TENG at humidity 95 %:
a – open circuit output voltage (V_{oc}); *b* – closed circuit output current (I_{sc})

The increase in RDF-TENG output voltage and current is caused by the formation of hydrogen bonds between hydroxyl groups and water molecules (when humidity is high) on the surface of the CS-PVA/TiO_2 nanocomposite film increasing the positive triboelectrification properties of the film. This is not much different from the research reported by Wang et al. using starch polymers rich in hydroxyl groups with the formation of hydrogen bonds with water molecules when humidity is high can increase the output current of RDF-TENG based starch films [45]. PVA film is rich in hydroxyl chains and can increase the number of hydroxyl chains when mixed with starch molecules. In this case, it can bind more water molecules when the humidity is high and increase participation in triboelectric charging. The results of this study are also in line with previous studies using hydroxyl-rich biofilms, at high humidity of 95 % a water molecule bonds with the hydroxyl through hydrogen bonds, which increases the generation of charge when the two films rub together and increases RDF-TENG work [46].

3. 6. Limitations of the study and development prospects

The limitations of the CS/PVA-TiO_2 nanocomposite film study are still limited to the physicochemical properties of the film to overcome the reduced performance of solid-solid TENG under high humidity conditions by increasing the hydroxyl groups that can bind water vapor molecules through hydrogen bonding, and increasing the density of the film by using TiO_2 fillers for increased absorption of water molecules. However, the tribological performance of CS/PVA-TiO_2 nanocomposite film when the relative humidity is high has not been studied in detail. This is important to do as a parameter of the durability of the CS/PVA-TiO_2 nanocomposite film as a triboelectric nanogenerator (TENG) friction film. The direction of further development studies can examine the tribological properties of CS/PVA-TiO_2 nanocomposite films that tend to be hydrophilic, such as; the effect of TiO_2 fillers in the CA/PVA composite matrix on the level of surface roughness, and the effect of relative humidity on the coefficient of friction, mass loss, short circuit current, and open circuit voltage for the surface of CS/PVA-TiO_2 nanocomposite films.

4. Conclusions

We developed a cassava starch (CS)/PVA-TiO_2 nanocomposite film using the solvent casting method for the application of the RDF-TENG triboelectric film. The addition of TiO_2 to the CS/PVA polymer composite from the SEM and XRD tests showed that the TiO_2 nanoparticles were evenly incorporated into the CS/PVA polymer matrix, and affected the crystal structure of the film. In addition, the presence of TiO_2 nanoparticles in the CS/PVA polymer resulted in an increase in Tensile Strength of 19.11 MPa for a 0.5 % wt. TiO_2 sample, and an optimal Tensile Strength of 21.20 MPa with a concentration of 1 % wt TiO_2 but the elongation at break value of the nanocomposite film CS/PVA-TiO_2 decreased. In addition, the effect of TiO_2 particles increases water resistance and decreases water wettability with an increase in the water contact angle of 83.60 at a concentration of 7 % wt TiO_2 which means an increase in hydrophobic properties. The performance of RDF-TENG films without the addition of TiO_2 on the CS-PVA nanocomposite matrix resulted in an output voltage and current of ~25.5 V and ~3.6 μA, and the performance RDF-TENG increased optimally with the addition of 3 % TiO_2 with an increase in the output voltage of 4.4-fold, and current 2.8-fold while performance under different humidity conditions (15 % and 95 % RH) output voltage increased 1.6-fold and current increased 1.4-fold with output voltage and current from ~112.5 V to ~180 V and current respectively from ~10.2 μA to ~13.7 μA. The increase was caused by the interaction of hydroxyl groups and water molecules through hydrogen bonds and the availability of free oxygen due to the distribution of TiO_2 particles, which increased the positive triboelectrification properties of the film. The performance of RDF TENG with low rotation and small torque has shown a relatively constant conversion efficiency. This is different from other rotational power generation machines, such as electromagnetic generators (EMG) which require high rotation and large torque to improve conversion efficiency. This provides an alternative solution for energy conversion models especially low mechanical energy by using triboelectric nanogenerator models.

Conflict of interest

The authors declare no conflict of interest. The funders had no role in research design; in the collection, analysis, or interpretation of data, in the writing of the manuscript, which may influence the work, reported in this paper, or in the decision to publish its results.

Financing

This work is supported and funded by the Institute for Research and Community Service, Universitas Negeri Surabaya (Unesa), with a grant contract number B/37502/2022.

Data availability

Manuscript has data included as electronic supplementary material, in a data repository; https://github.com/arisansori/Supplementary-Materials-.git

Acknowledgements

We gratefully acknowledge the support of the Surabaya State University (Unesa) Research and Community Service Institute, for research funding with a grant contract number: B/37502/2022. We are also grateful for the technical support from the Energy Conversion Laboratory at the Department of Mechanical Engineering, University Brawijaya, Central Laboratory of Life Sciences, University Brawijaya, and Advanced Mineral & Material Central Laboratory FMIPA, State University of Malang.

References

[1] Dzhardimalieva, G. I., Yadav, B. C., Lifintseva, T. V., Uflyand, I. E. (2021). Polymer chemistry underpinning materials for triboelectric nanogenerators (TENGs): Recent trends. European Polymer Journal, 142, 110163. doi: https://doi.org/10.1016/j.eurpolymj.2020.110163

[2] Wang, J., Wu, C., Dai, Y., Zhao, Z., Wang, A., Zhang, T., Wang, Z. L. (2017). Achieving ultrahigh triboelectric charge density for efficient energy harvesting. Nature Communications, 8 (1). doi: https://doi.org/10.1038/s41467-017-00131-4

[3] Xia, K., Fu, J., Xu, Z. (2020). Multiple-Frequency High-Output Triboelectric Nanogenerator Based on a Water Balloon for All-Weather Water Wave Energy Harvesting. Advanced Energy Materials, 10 (28), 2000426. doi: https://doi.org/10.1002/aenm.202000426

[4] Song, G., Kim, Y., Yu, S., Kim, M.-O., Park, S.-H., Cho, S. M. et al. (2015). Molecularly Engineered Surface Triboelectric Nanogenerator by Self-Assembled Monolayers (METS). Chemistry of Materials, 27 (13), 4749–4755. doi:https://doi.org/10.1021/acs.chemmater.5b01507

[5] Mallakpour, S., Jarang, N. (2015). Mechanical, thermal and optical properties of nanocomposite films prepared by solution mixing of poly (vinyl alcohol) with titania nanoparticles modified with citric acid and vitamin C. Journal of Plastic Film & Sheeting, 32 (3), 293–316. doi: https://doi.org/10.1177/8756087915597024

[6] Khushboo, Azad, P. (2018). Design and Implementation of Conductor-to-Dielectric Lateral Sliding TENG Mode for Low Power Electronics. Applications of Artificial Intelligence Techniques in Engineering, 167–174. doi: https://doi.org/10.1007/978-981-13-1819-1_17

[7] Park, H.-W., Huynh, N. D., Kim, W., Lee, C., Nam, Y., Lee, S., Chung, K.-B., Choi, D. (2018). Electron blocking layer-based interfacial design for highly-enhanced triboelectric nanogenerators. Nano Energy, 50, 9–15. doi: https://doi.org/10.1016/j.nanoen.2018.05.024

[8] Trihutomo, P., Marji, M., Harly, M., Wahyudi, B. A., Radja, M. B. (2022). The effect of Clathrin protein addition on increasing the number of electrons in organic Dye-Sensitized Solar Cell (DSSC). EUREKA: Physics and Engineering, 2, 15–27. doi: https://doi.org/10.21303/2461-4262.2022.001957

[9] Kum-onsa, P., Chanlek, N., Manyam, J., Thongbai, P., Harnchana, V., Phromviyo, N., Chindaprasirt, P. (2021). Gold-Nanoparticle-Deposited TiO2 Nanorod/Poly(Vinylidene Fluoride) Composites with Enhanced Dielectric Performance. Polymers, 13 (13), 2064. doi: https://doi.org/10.3390/polym13132064

[10] Huynh, N. D., Park, H., Chung, K., Choi, D. (2018). Effect on TENG Performance by Phase Control of TiOx Nanoparticles. Composites Research, 31 (6), 365–370. doi: https://doi.org/10.7234/composres.2018.31.6.365

[11] Bunriw, W., Harnchana, V., Chanthad, C., Huynh, V. N. (2021). Natural Rubber-TiO2 Nanocomposite Film for Triboelectric Nanogenerator Application. Polymers, 13 (13), 2213. doi: https://doi.org/10.3390/polym13132213

[12] Wang, Y., Zhang, L., Lu, A. (2020). Highly stretchable, transparent cellulose/PVA composite hydrogel for multiple sensing and triboelectric nanogenerators. Journal of Materials Chemistry A, 8 (28), 13935–13941. doi: https://doi.org/10.1039/d0ta02010a

[13] Shi, K., Huang, X., Sun, B., Wu, Z., He, J., Jiang, P. (2019). Cellulose/$BaTiO_3$ aerogel paper based flexible piezoelectric nanogenerators and the electric coupling with triboelectricity. Nano Energy, 57, 450–458. doi: https://doi.org/10.1016/j.nanoen.2018.12.076

[14] Chen, X., Yusuf, A., del Rio, J. S., Wang, D.-Y. (2021). A facile and robust route to polyvinyl alcohol-based triboelectric nanogenerator containing flame-retardant polyelectrolyte with improved output performance and fire safety. Nano Energy, 81, 105656. doi: https://doi.org/10.1016/j.nanoen.2020.105656

[15] Singh, R., Rhee, H.-W. (2019). The rise of bio-inspired energy devices. Energy Storage Materials, 23, 390–408. doi: https://doi.org/10.1016/j.ensm.2019.04.030

[16] Zhu, Z., Xia, K., Xu, Z., Lou, H., Zhang, H. (2018). Starch Paper-Based Triboelectric Nanogenerator for Human Perspiration Sensing. Nanoscale Research Letters, 13 (1). doi: https://doi.org/10.1186/s11671-018-2786-9

[17] Chi, Y., Xia, K., Zhu, Z., Fu, J., Zhang, H., Du, C., Xu, Z. (2019). Rice paper-based biodegradable triboelectric nanogenerator. Microelectronic Engineering, 216, 111059. doi: https://doi.org/10.1016/j.mee.2019.111059

[18] Gots, V., Palchyk, P., Berdnyk, O. (2018). Investigation of properties of modified basalt fibers. EUREKA: Physics and Engineering, 4, 43–48. doi: https://doi.org/10.21303/2461-4262.2018.00673

[19] Ccorahua, R., Huaroto, J., Luyo, C., Quintana, M., Vela, E. A. (2019). Enhanced-performance bio-triboelectric nanogenerator based on starch polymer electrolyte obtained by a cleanroom-free processing method. Nano Energy, 59, 610–618. doi: https://doi.org/10.1016/j.nanoen.2019.03.018

[20] Shi, L., Dong, S., Xu, H., Huang, S., Ye, Q., Liu, S. et al. (2019). Enhanced performance triboelectric nanogenerators based on solid polymer electrolytes with different concentrations of cations. Nano Energy, 64, 103960. doi: https://doi.org/10.1016/j.nanoen.2019.103960

[21] Shen, J., Li, Z., Yu, J., Ding, B. (2017). Humidity-resisting triboelectric nanogenerator for high performance biomechanical energy harvesting. Nano Energy, 40, 282–288. doi: https://doi.org/10.1016/j.nanoen.2017.08.035

[22] Ccorahua, R., Cordero, A., Luyo, C., Quintana, M., Vela, E. (2019). Starch-Cellulose-Based Triboelectric Nanogenerator Obtained by a Low-Cost Cleanroom-Free Processing Method. MRS Advances, 4 (23), 1315–1320. doi: https://doi.org/10.1557/adv.2018.652

[23] Torres, F. G., Troncoso, O. P., Torres, C., Díaz, D. A., Amaya, E. (2011). Biodegradability and mechanical properties of starch films from Andean crops. International Journal of Biological Macromolecules, 48 (4), 603–606. doi: https://doi.org/10.1016/j.ijbiomac.2011.01.026

[24] Kim, J.-Y., Choi, Y.-G., Byul Kim, S. R., Lim, S.-T. (2014). Humidity stability of tapioca starch-pullulan composite films. Food Hydrocolloids, 41, 140–145. doi: https://doi.org/10.1016/j.foodhyd.2014.04.008

[25] Ben Doudou, B., Vivet, A., Chen, J., Laachachi, A., Falher, T., Poilâne, C. (2014). Hybrid carbon nanotube-silica/ polyvinyl alcohol nanocomposites films: preparation and characterisation. Journal of Polymer Research, 21 (4). doi: https://doi.org/10.1007/s10965-014-0420-9

[26] Fei, P., Shi, Y., Zhou, M., Cai, J., Tang, S., Xiong, H. (2013). Effects of nano-TiO2on the properties and structures of starch/poly(ε-caprolactone) composites. Journal of Applied Polymer Science. doi: https://doi.org/10.1002/app.39695

[27] Alvarez-Ramirez, J., Vazquez-Arenas, J., García-Hernández, A., Vernon-Carter, E. J. (2019). Improving the mechanical performance of green starch/glycerol/Li+ conductive films through cross-linking with Ca2+. Solid State Ionics, 332, 1–9. doi: https://doi.org/10.1016/j.ssi.2019.01.002

[28] Zamanian, M., Sadrnia, H., Khojastehpour, M., Hosseini, F., Thibault, J. (2021). Effect of TiO_2 nanoparticles on barrier and mechanical properties of PVA films. Journal of Membrane Science and Research, 7 (2), 67–73. doi: https://doi.org/10.22079/JMSR.2020.112911.1283

[29] Kochkina, N. E., Butikova, O. A. (2019). Effect of fibrous TiO2 filler on the structural, mechanical, barrier and optical characteristics of biodegradable maize starch/PVA composite films. International Journal of Biological Macromolecules, 139, 431–439. doi: https://doi.org/10.1016/j.ijbiomac.2019.07.213

[30] Oleyaei, S. A., Almasi, H., Ghanbarzadeh, B., Moayedi, A. A. (2016). Synergistic reinforcing effect of TiO2 and montmorillonite on potato starch nanocomposite films: Thermal, mechanical and barrier properties. Carbohydrate Polymers, 152, 253–262. doi: https://doi.org/10.1016/j.carbpol.2016.07.040

[31] Abdullah, A. M., Aziz, S. B., Saeed, S. R. (2021). Structural and electrical properties of polyvinyl alcohol (PVA):Methyl cellulose (MC) based solid polymer blend electrolytes inserted with sodium iodide (NaI) salt. Arabian Journal of Chemistry, 14(11), 103388. doi: https://doi.org/10.1016/j.arabjc.2021.103388

[32] Adamu, A. D., Jikan, S. S., Talip, B. H. A., Badarulzaman, N. A., Yahaya, S. (2017). Effect of Glycerol on the Properties of Tapioca Starch Film. Materials Science Forum, 888, 239–243. doi: https://doi.org/10.4028/www.scientific.net/msf.888.239

[33] Abral, H., Hartono, A., Hafizulhaq, F., Handayani, D., Sugiarti, E., Pradipta, O. (2019). Characterization of PVA/cassava starch biocomposites fabricated with and without sonication using bacterial cellulose fiber loadings. Carbohydrate Polymers, 206, 593–601. doi: https://doi.org/10.1016/j.carbpol.2018.11.054

[34] Surudžić, R., Janković, A., Bibić, N., Vukašinović-Sekulić, M., Perić-Grujić, A., Mišković-Stanković, V. et al. (2016). Physico-chemical and mechanical properties and antibacterial activity of silver/poly(vinyl alcohol)/graphene nanocomposites obtained by electrochemical method. Composites Part B: Engineering, 85, 102–112. doi: https://doi.org/10.1016/j.compositesb.2015.09.029

[35] Tian, H., Yan, J., Rajulu, A. V., Xiang, A., Luo, X. (2017). Fabrication and properties of polyvinyl alcohol/starch blend films: Effect of composition and humidity. International Journal of Biological Macromolecules, 96, 518–523. doi: https://doi.org/10.1016/j.ijbiomac.2016.12.067

[36] Patil, S., Bharimalla, A. K., Mahapatra, A., Dhakane-Lad, J., Arputharaj, A., Kumar, M. et al. (2021). Effect of polymer blending on mechanical and barrier properties of starch-polyvinyl alcohol based biodegradable composite films. Food Bioscience, 44, 101352. doi: https://doi.org/10.1016/j.fbio.2021.101352

[37] Garbuz, A., Bilym, P., Zubenko, D. (2016). Features of changes of structure and adhesive properties for acrylic adhesives under the influence of the filler. EUREKA: Physics and Engineering, 3, 13–16. doi: https://doi.org/10.21303/2461-4262.2016.00075

[38] Khalaf, A. A., Abed, S. A., Alkhfaji, S. S., Al-Obaidi, M. A., Hanon, M. M. (2022). The effect of adding natural materials waste on the mechanical properties and water absorption of epoxy composite using grey relations analysis. EUREKA: Physics and Engineering, 1, 131–142. doi: https://doi.org/10.21303/2461-4262.2022.001952

[39] Ji, M., Li, F., Li, J., Li, J., Zhang, C., Sun, K., Guo, Z. (2021). Enhanced mechanical properties, water resistance, thermal stability, and biodegradation of the starch-sisal fibre composites with various fillers. Materials & Design, 198, 109373. doi: https://doi.org/10.1016/j.matdes.2020.109373

[40] Bergo, P., Sobral, P. J. A., Prison, J. M. (2010). Effect of glycerol on physical properties of cassava starch films. Journal of Food Processing and Preservation, 34, 401–410. doi: https://doi.org/10.1111/j.1745-4549.2008.00282.x

[41] Wang, Y., Zhang, H., Zeng, Y., Hossen, M. A., Dai, J., Li, S. et al. (2022). Development and characterization of potato starch/lactucin/nano-TiO_2 food packaging for sustained prevention of mealworms. Food Packaging and Shelf Life, 33, 100837. doi: https://doi.org/10.1016/j.fpsl.2022.100837

[42] Sintusiri, J., Harnchana, V., Amornkitbamrung, V., Wongsa, A., Chindaprasirt, P. (2020). Portland Cement-TiO_2 triboelectric nanogenerator for robust large-scale mechanical energy harvesting and instantaneous motion sensor applications. Nano Energy, 74, 104802. doi: https://doi.org/10.1016/j.nanoen.2020.104802

[43] Park, H.-W., Huynh, N., Kim, W., Hwang, H., Hong, H., Choi, K. et al. (2018). Effects of Embedded $TiO_2{-}x$ Nanoparticles on Triboelectric Nanogenerator Performance. Micromachines, 9 (8), 407. doi: https://doi.org/10.3390/mi9080407

[44] Rong, L., Shen, M., Wen, H., Ren, Y., Xiao, W., Xie, J. (2021). Preparation and characterization of hyacinth bean starch film incorporated with TiO2 nanoparticles and Mesona chinensis Benth polysaccharide. International Journal of Biological Macromolecules, 190, 151–158. doi: https://doi.org/10.1016/j.ijbiomac.2021.08.180

[45] Wang, N., Feng, Y., Zheng, Y., Zhang, L., Feng, M., Li, X. et al. (2021). New Hydrogen Bonding Enhanced Polyvinyl Alcohol Based Self-Charged Medical Mask with Superior Charge Retention and Moisture Resistance Performances. Advanced Functional Materials, 31(14), 2009172. doi: https://doi.org/10.1002/adfm.202009172

[46] Wang, N., Zheng, Y., Feng, Y., Zhou, F., Wang, D. (2020). Biofilm material based triboelectric nanogenerator with high output performance in 95 % humidity environment. Nano Energy, 77, 105088. doi: https://doi.org/10.1016/j.nanoen.2020.105088

Received date 08.11.2022
Accepted date 12.03.2023
Published date 22.03.2023

How to cite: *Ansori, A., Soeparman, S., Widhiyanuriyawan, D., Widodo, T. D. (2023). Enhanced mechanical and water resistance properties of cassava starch-PVA nanocomposites with TiO_2 nanofillers for triboelectric nanogenerators films. EUREKA: Physics and Engineering, 2, 184–201. doi: https://doi.org/10.21303/2461-4262.2023.002647*

ENHANCED MECHANICAL AND WATER RESISTANCE PROPERTIES OF CASSAVA STARCH-PVA NANOCOMPOSITES WITH TiO2 NANOFILLERS FOR TRIBOELECTRIC NANOGENERATORS FILMS

ORIGINALITY REPORT

7%	2%	9%	5%
SIMILARITY INDEX	INTERNET SOURCES	PUBLICATIONS	STUDENT PAPERS

PRIMARY SOURCES

1	Nikolai Kobasko, Anatolii Moskalenko, Volodymyr Dobryvechir. "RESEARCH ON USE OF LOW CONCENTRATION INVERSE SOLUBILITY POLYMERS IN WATER FOR HARDENING MACHINE COMPONENTS AND TOOLS", EUREKA: Physics and Engineering, 2018 Publication	1%
2	Yue Wang, Haitian Zhang, Yuanbo Zeng, Md Alomgir Hossen, Jianwu Dai, Suqing Li, Yaowen Liu, Wen Qin. "Development and characterization of potato starch/lactucin/nano-TiO2 food packaging for sustained prevention of mealworms", Food Packaging and Shelf Life, 2022 Publication	1%
3	Oranooch Somseemee, Pongdhorn Sae-Oui, Chomsri Siriwong. "Bio-based epoxidized natural rubber/chitosan/cellulose nanocrystal	1%

composites for enhancing mechanical properties, self-healing behavior and triboelectric nanogenerator performance", Cellulose, 2022
Publication

---

4 Aris Ansori, Teguh Dwi Widodo, Sudjito Soeparman, Denny Widhiyanuriyawan. "Enhanced Performance Triboelectric Nanogenerator With Strach Biopolymer Composite Interface Layer", 2021 3rd International Conference on Research and Academic Community Services (ICRACOS), 2021 — 1 %
Publication

---

5 Veronika Cherkashyna. "ANALYSIS OF PARAMETERS SERIES OF WIRE CROSS-SECTIONS FOR OVERHEAD POWER LINE DESIGN", EUREKA: Physics and Engineering, 2016 — 1 %
Publication

---

6 Nannan Wang, Yange Feng, Youbin Zheng, Liqiang Zhang, Min Feng, Xiaojuan Li, Feng Zhou, Daoai Wang. "New Hydrogen Bonding Enhanced Polyvinyl Alcohol Based Self - Charged Medical Mask with Superior Charge Retention and Moisture Resistance Performances", Advanced Functional Materials, 2021 — 1 %
Publication

7	K. Rajesh, Vincent Crasta, N. B. Rithin Kumar, Gananatha Shetty, P. D. Rekha. "Structural, optical, mechanical and dielectric properties of titanium dioxide doped PVA/PVP nanocomposite", Journal of Polymer Research, 2019 Publication	1 %
8	Submitted to Thammasat University Student Paper	1 %
9	www.journal.eu-jr.eu Internet Source	1 %
10	Submitted to Universiti Malaysia Pahang Student Paper	1 %

Exclude quotes	Off	Exclude matches	< 1%
Exclude bibliography	Off		